Electric field induced instabilities: Waves and stationary patterns

Sumana Dutta and Deb Shankar Ray*
Indian Association for the Cultivation of Science, Jadavpur, Calcutta 700 032, India
(Received 6 October 2005; published 15 February 2006)

We examine a prototypical ionic reaction-diffusion system involving the well-known iodate-arsenous acid reaction in an electric field at a constant current density. By taking into consideration of the spatial inhomogeneities in electric field intensity and charge density due to ionic migration and diffusion using charge balance condition, we look for the different instability regions in the appropriate parameter space. We show that the model admits of both absolute and convective instability resulting in the development of propagating waves and also stationary spatial patterns at times.

DOI: 10.1103/PhysRevE.73.026210 PACS number(s): 05.45.−a, 82.20.Uv, 82.45.−h

I. INTRODUCTION

The interaction between diffusion and nonlinearity in many natural processes often bring about spatiotemporal and stationary pattern formation in spatially extended systems, when the later is driven out of equilibrium. For ionic components of a reaction medium electric field plays an important role in migration and transport of ions [1]. Whether in the arena of ionic reactions, cardiac activity, nonlinear optics, electrophoresis, morphogenesis, cell biology, fractal formation in colloids, polymerization or nervous stimuli, electric field effects are wide and many in the context of chemical wave propagation and stationary pattern formation [2–8].

The study of electric field effects in reaction-diffusion systems can be dated back to the early works of Ortoleva *et al.* [2,9,10]. Chemical waves are stopped, annihilated, and aggravated by electric fields. Formation of multiple waves and hysteric effects due to the nonlinear dependence on the field have been studied in detail. In addition to the changes in velocity of propagation of traveling wave fronts, the effect of externally applied electric fields have also been found to be behind the reversal and splitting of waves in an excitable system [1,11] and the formation of stationary patterns [12]. Extensive numerical and experimental works, mostly related to the Belousov-Zhabotinsky reaction have been reported in this context. In a majority of these studies, the applied electric field is homogeneous in nature. This approximation neglects the local inhomogeneity of the electric field intensity and charge density arising due to differences in mobilities of the ions. For a medium with low ionic strength and low mobility, it has been realized that one must take into account of the local inhomogeneities of the field and charge density for fast reactions (a commonly occurring situation for ionic reactions). This could be done by appropriately employing charge balance condition [13] using the Nernst-Planck equation. To this end, the effect of spatial inhomogeneities in electric field intensity and charge density due to interaction of diffusion with chemical reaction was first demonstrated in the Brusselator model [14].

In this paper we are concerned with a planar reaction diffusion system driven by an inhomogeneous electric field but at a constant current density under a charge balance condition. The motivation behind the present study is the following: in absence of electric field, electric potential is primarily due to ionic diffusion. On the other hand, in presence of the externally applied field, a stronger field is likely to develop around the reacting zone when a constant current density is maintained under a charge balance condition. This is because the condition of constancy of current density is expected to produce more ions [1] as a result of chemical reaction due to stoichiometric requirement. In the process, one may expect the onset of instability resulting in wave propagation and stationary pattern formation. We undertake the present study by considering a general prototypical model of the iodate-arsenous acid reaction. Our aim is twofold.

(i) To explore the signature of instability and its consequences due to inhomogeneous electric field under a charge balance condition. We identify several regions of instability to demonstrate absolute as well as convective instabilities, resulting in wave propagation and also the formation of stationary pattern.

(ii) Although the iodate-arsenous acid system has been the experimental testing ground of a number of prototypical studies on wave propagation, the application of charge balance condition using the Nernst-Planck equation and consideration of inhomogeneties in electric field intensity has not been investigated in this system.

We corroborate our theoretical analysis by numerical simulations on the reaction-diffusion system in two dimensions.

II. THE MODEL

We have chosen to deal with one of the simplest of different chemical systems that has been widely undertaken by numerous groups over the last three decades for the study of wave-front propagation and noise induced instability, the arsenous acid-iodate reaction [15,16]. Detailed studies made by Showalter and co-workers [17] have portrayed the varied wave front characteristics of this reaction. Different experimental and numerical works analyzing the dependence of wave-front velocity on the stoichiometry and the ratio of diffusivities of autocatalyst and reactants in this system have been carried out [18,19]. Experimental studies have shown

*Email address: pcdsr@mahendra.iacs.res.in

that externally applied electric fields and the subsequent influence of starch indicator are instrumental in altering the propagation velocity of the wave as well as the front characteristics [20,21].

The arsenous acid-iodate system is a composite of two reactions, viz. the Dushman reaction (2.1) and the Roebuck reaction (2.2), which have been known for over a century [22,23]

$$IO_3^- + 5I^- + 6H^+ \leftrightharpoons 3I_2 + 3H_2O, \tag{2.1}$$

$$H_3AsO_3 + I_2 + H_2O \rightarrow H_3AsO_4 + 2I^- + 2H^+. \tag{2.2}$$

In the overall process, the Dushman reaction is the rate determining step [17,24]. We have here followed the kinetic studies of the later as given by Schmitz [25], where the experimental observation of the simultaneous first and second order dependence of the rate on $[I^-]$ over a range of low to moderately low concentration of I^- has been made. The rate law for the system is given by

$$\frac{d[I^-]}{dt} = (k_1 + k_2[I^-])[I^-][IO_3^-][H^+]^2, \tag{2.3}$$

where $k_1 = 4.5 \times 10^5\ M^{-3}\ s^{-1}$ and $k_2 = 1.0 \times 10^8\ M^{-4}\ s^{-1}$ are the experimental rate constants.

The conspicuous feature of this reaction is the role of I_2 as an intermediate. The sharp change in the concentration of the iodine containing species, viz. I^-, IO_3^-, and I_2 as functions of time in a stirred batch reactor is another interesting characteristic of this reaction. This allows the assumption that all the iodine is either present as I^- or IO_3^-, the concentration of I_2 being negligible as compared to these two species [26]. Furthermore rapidity of the reaction step, as emphasized by Münster *et al.* [14], invalidates the condition of the assumption of homogeneous electric field.

The present study begins with a note that when the system is spatially extended, a sharp change in concentration of iodine-containing species with time is likely to make the spatial local gradient of these species appreciably sharp. This, as well as the difference in mobilities of the ionic species result in local inhomogeneity of electric field intensity and electric charge density in the reaction medium. It is thus pertinent to consider the variation in electric potential gradient $\nabla\phi$ explicitly by taking into consideration of the charge balance condition.

Keeping in view of these discussions, we have the following rate equations for the three ionic species $[I^-]$, $[IO_3^-]$, and $[H^+]$, respectively:

$$\frac{d[I^-]}{dt} = (k_1 + k_2[I^-])[I^-][IO_3^-][H^+]^2 - \nabla \cdot J_{[I^-]}, \tag{2.4}$$

$$\frac{d[IO_3^-]}{dt} = -\nabla \cdot J_{[IO_3^-]}, \tag{2.5}$$

$$\frac{d[H^+]}{dt} = -\nabla \cdot J_{[H^+]}, \tag{2.6}$$

where J_i denotes the flux of the ith ionic species for the system.

For a reaction diffusion system, in the presence of an inhomogeneous charge density, the flux for an ionic species is given by the Nernst-Planck equation [27], viz.

$$\mathbf{J_i} = -D_i \nabla C_i - \frac{D_i z_i F}{RT} C_i \nabla \phi, \tag{2.7}$$

where D_i denotes the diffusion coefficient. z_i is the charge on the ion i, in atomic units (with sign), C_i is the concentration in M ($mol\ dm^{-3}$) of the ith ion, and T is the absolute temperature. R and F denote the universal gas constant and the Faraday's constant in S.I. units, respectively. Here, ϕ stands for the electric potential and

$$-\frac{F}{RT} \nabla \phi = \mathbf{E}, \tag{2.8}$$

E being the electric field or the electric potential gradient in dimensions of L^{-1}. Thus, Eq. (2.7) takes the following form:

$$\mathbf{J_i} = -D_i \nabla C_i + D_i z_i C_i \mathbf{E}. \tag{2.9}$$

Now we substitute $u(x,y,t)$, $v(x,y,t)$, and $w(x,y,t)$ for $[I^-]$, $[IO_3^-]$, and $[H^+]$, respectively. Considering $D_{I^-} = D_{IO_3^-} = D_{H^+}/d = 1$, with $d = 2$, we obtain the following forms of the rate equations:

$$\frac{\delta u(x,y,t)}{\delta t} = -(k_1 + k_2 u)uvw^2 + \nabla \cdot (\nabla u + u\mathbf{E}), \tag{2.10}$$

$$\frac{\delta v(x,y,t)}{\delta t} = \nabla \cdot (\nabla v + v\mathbf{E}), \tag{2.11}$$

$$\frac{\delta w(x,y,t)}{\delta t} = d\nabla \cdot (\nabla w - w\mathbf{E}). \tag{2.12}$$

To look into the electrical inhomogeneities of the reaction medium we first derive the expression for the local field E. To this end we consider the total electric current density as given by

$$\mathbf{I} = \sum_i F z_i \mathbf{J_i}. \tag{2.13}$$

A charge balance condition implies

$$\nabla \cdot \mathbf{I} = \mathbf{0} \tag{2.14}$$

which yields

$$\nabla \cdot \sum_i z_i \mathbf{J_i} = 0. \tag{2.15}$$

This implies

$$\sum_i z_i \mathbf{J_i} = \text{const} = \mathbf{j}(say). \tag{2.16}$$

We now put the expression for J_i from Eqs. (2.9) into (2.16) to obtain

$$\sum_i (-D_i z_i \nabla C_i + D_i z_i^2 C_i \mathbf{E}) = \mathbf{j}, \tag{2.17}$$

E can now be expressed as

$$\mathbf{E} = \frac{\mathbf{j} + \sum_i D_i z_i \nabla C_i}{\sum_i D_i z_i^2 C_i}. \tag{2.18}$$

The above equation when rewritten in terms of the concentration of the ionic species u, v, w gives us the expression for the electric field:

$$\mathbf{E} = \frac{\mathbf{j} - \nabla u - \nabla v + d \nabla w}{u + v + dw}. \tag{2.19}$$

This expression obtained directly from the Nernst-Planck equation under the charge balance condition describes the local electrical inhomogeneities of the medium. During spatio-temporal evolution of the reaction-diffusion system (2.10)–(2.12), the potential field or the inhomogeneous electric field, has to be recalculated each time.

III. LINEAR STABILITY ANALYSIS

We assume the existence of a spatially uniform steady state ($u=u_0$, $v=v_0$, $w=w_0$), of the dynamical system, such that

$$f(u_0, v_0, w_0) = 0, \tag{3.1}$$

where $f(u,v,w)$ denotes the reaction part of Eq. (2.10). We furthermore assume that this state is stable in absence of diffusion., i.e.,

$$\left[\frac{\delta f}{\delta u}\right]_{u=u_0, v=v_0, w=w_0} = f' < 0. \tag{3.2}$$

The above condition admits of three steady states of the dynamics, viz., $u_0=-k_1/k_2$, $u_0=0$, and $v_0=0$. The stability of the steady state as implied in Eq. (3.2) is purely kinetic in nature. Since we are interested in the stable homogeneous steady state it is also necessary to ensure that the choice of parameter space does not lead to instability when diffusion ratio is incorporated in the analysis.

Considering an expansion of u, v and w in Eq. (2.10) about the steady value (u_0, v_0, w_0) we have

$$\frac{\delta(u_0+\delta\bar{u})}{\delta\tau} = f(u_0+\delta\bar{u}, v_0+\delta\bar{v}, w_0+\delta\bar{w}) + \nabla_{x,y}^2(u_0+\delta\bar{u}) + \nabla_x(u_0+\delta\bar{u})\left[\frac{j - \nabla(u_0+\delta\bar{u}) - \nabla(v_0+\delta\bar{v}) + d\nabla(w_0+\delta\bar{w})}{(u_0+v_0+dw_0)+(\delta\bar{u}+\delta\bar{v}+d\delta\bar{w})}\right]. \tag{3.3}$$

Expanding f in a Taylor series about the steady value and employing a Binomial expansion to the term due to E, while considering only the linear terms in $\delta\bar{u}$, $\delta\bar{v}$, $\delta\bar{w}$, we have

$$\begin{aligned}\frac{\delta(\delta\bar{u})}{\delta t} &= -v_0 w_0^2 k_1 \delta\bar{u} - u_0 w_0^2 k_1 \delta\bar{v} - 2u_0 v_0 w_0 k_1 \delta\bar{w} \\ &\quad - 2u_0 v_0 w_0^2 k_2 \delta\bar{u} - u_0^2 w_0^2 k_2 \delta\bar{v} - 2u_0^2 v_0 w_0 k_2 \delta\bar{w} + \nabla_{x,y}^2 \delta\bar{u} \\ &\quad - \frac{u_0 j}{a_0^2}\nabla_x(\delta\bar{u}+\delta\bar{v}+d\delta\bar{w}) - \frac{u_0}{a_0}\nabla_x^2(\delta\bar{u}+\delta\bar{v}-d\delta\bar{w}) \\ &\quad + \frac{j}{a_0}\nabla_x\delta\bar{u}.\end{aligned} \tag{3.4}$$

Here the constant sum $(u_0+v_0+dw_0)$ has been replaced by another constant a_0, for the purpose of simplicity. Proceeding similarly Eqs. (2.11) and (2.12) take the form

$$\begin{aligned}\frac{\delta(\delta\bar{v})}{\delta t} &= \nabla_{x,y}^2\delta\bar{v} - \frac{v_0 j}{a_0^2}\nabla_x(\delta\bar{u}+\delta\bar{v}+d\delta\bar{w}) \\ &\quad - \frac{v_0}{a_0}\nabla_x^2(\delta\bar{u}+\delta\bar{v}-d\delta\bar{w}) + \frac{j}{a_0}\nabla_x\delta\bar{v},\end{aligned} \tag{3.5}$$

$$\begin{aligned}\frac{\delta(\delta\bar{w})}{\delta t} &= d\nabla_{x,y}^2\delta\bar{w} + \frac{dw_0 j}{a_0^2}\nabla_x(\delta\bar{u}+\delta\bar{v}+d\delta\bar{w}) \\ &\quad + \frac{dw_0}{a_0}\nabla_x^2(\delta\bar{u}+\delta\bar{v}-d\delta\bar{w}) - \frac{dj}{a_0}\nabla_x\delta\bar{w}.\end{aligned} \tag{3.6}$$

We now express the spatiotemporal perturbations as

$$\delta\bar{u}(x,y,t) = Ae^{i(k_x x + k_y y - \omega t)}, \tag{3.7}$$

$$\delta\bar{v}(x,y,t) = Be^{i(k_x x + k_y y - \omega t)}, \tag{3.8}$$

$$\delta\bar{w}(x,y,t) = Ce^{i(k_x x + k_y y - \omega t)}, \tag{3.9}$$

where A, B, and C are constants.

Substituting the above into Eqs. (3.4)–(3.6), we have

$$\begin{aligned}-i\omega A &= -(v_0 w_0^2 k_1 + 2u_0 v_0 w_0^2 k_2)A \\ &\quad - (u_0 w_0^2 k_1 + u_0^2 w_0^2 k_2)B - 2(u_0 v_0 w_0 k_1 + u_0^2 v_0 w_0 k_2)C \\ &\quad - (k_x^2 + k_y^2)A - \frac{iu_0 j k_x}{a_0^2}(A+B+dC) \\ &\quad + \frac{u_0 k_x^2}{a_0}(A+B-dC) + \frac{ijk_x}{a_0}A\end{aligned} \tag{3.10}$$

$$-i\omega B = -(k_x^2 + k_y^2)B - \frac{iv_0 jk_x}{a_0^2}(A + B + dC) + \frac{v_0 k_x^2}{a_0}(A + B - dC) + \frac{ijk_x}{a_0}B \tag{3.11}$$

$$-i\omega C = -d(k_x^2 + k_y^2)C + \frac{idw_0 jk_x}{a_0^2}(A + B + dC) - \frac{dw_0 k_x^2}{a_0}(A + B - dC) - \frac{idjk_x}{a_0}C. \tag{3.12}$$

The system of Eqs. (3.10)–(3.12) can be put in the form of a matrix equation as

$$L\begin{pmatrix} A \\ B \\ C \end{pmatrix} = 0, \tag{3.13}$$

where

$$L = \begin{pmatrix} l_{11} + i\omega & l_{12} & l_{13} \\ l_{21} & l_{22} + i\omega & l_{23} \\ l_{31} & l_{32} & l_{33} + i\omega \end{pmatrix}.$$

The detailed expressions of the elements of the above matrix are given in Appendix A.

To examine the stability, we now write the following determinantal equation for the eigenvalue problem

$$|L| = 0. \tag{3.14}$$

On expanding Eq. (3.14), we get the following dispersion relation, a cubic in ω:

$$(G_a\omega^2 + G_b\omega + G_c) + i(F_a\omega^3 + F_b\omega^2 + F_c\omega + F_d) = 0, \tag{3.15}$$

where G_a, G_b, and G_c are the real parts and F_a, F_b, F_c, and F_d are the imaginary parts of the coefficients of different powers of ω. Also $F_a = 1.0$. (For the cause of brevity, we have not mentioned the detailed expressions of the above coefficients.)

In order to obtain the variation of ω versus k_x, we find the group velocity, viz. $\delta\omega/\delta k_x$ by differentiating Eq. (3.15) by k_x:

$$\frac{\delta}{\delta k_x}[(G_a\omega^2 + G_b\omega + G_c) + i(\omega^3 + F_b\omega^2 + F_c\omega + F_d)] = 0. \tag{3.16}$$

We find the maxima of the group velocity at k_0 such that $[\delta\omega/\delta k_x]_{k_x=k_0} = 0$. Equation (3.16) takes the form

$$\omega^2(G^a_{k_0} + iF^b_{k_0}) + \omega(G^b_{k_0} + iF^c_{k_0}) + (G^c_{k_0} + iF^d_{k_0}) = 0, \tag{3.17}$$

where $G^a_{k_0} = [\delta G_a/\delta k_x]_{k_x=k_0}$, $G^b_{k_0} = [\delta G_b/\delta k_x]_{k_x=k_0}$, and so on.

By solving Eq. (3.17) we have

$$\omega_\pm = \frac{-(G^b_{k_0} + iF^c_{k_0}) \pm \sqrt{(G^b_{k_0} + iF^c_{k_0})^2 - 4(G^a_{k_0} + iF^b_{k_0})(G^c_{k_0} + iF^d_{k_0})}}{2(G^a_{k_0} + iF^b_{k_0})}. \tag{3.18}$$

Only those solutions of Eq. (3.17) that satisfy the dispersion relation, Eq. (3.15), are the required eigenvalues. Details of Eq. (3.18) are worked out in Appendix B.

We now look for the parameter spaces of the constant electric flux, j, versus the wave number k_0, for which the eigenvalues exist for a fixed value of k_y. The experimentally admissible parameters [26] are given by $k_1 = 4.5 \times 10^3$ M^{-3} s^{-1}; $k_2 = 1.0 \times 10^8$ M^{-4} s^{-1}; $D_{H^+} = 2 \times 10^{-1}$ mm^2 s^{-1}. And the initial conditions used are $u_0 = 6.0 \times 10^{-3}$ M; $v_0 = 0.0$ M; $w_0 = 7.1 \times 10^{-3}$ M. The nature of the eigenvalues in these spaces foretell the onset of instability in the presence of both negative as well as positive electric flux. Here we follow the same convention as chosen by Scott *et al.* [28], and distinguish between three typical situations. We may note that based on the nature of real and imaginary parts of $w(k_0)$ we have (i) $\mathrm{Re}[\omega(k_0)] \neq 0$, $\mathrm{Im}[\omega(k_0)] \neq 0$, absolute instability, (ii) $\mathrm{Re}[\omega(k_0)] \neq 0$, $\mathrm{Im}[\omega(k_0)] = 0$, convective instability, (iii) $\mathrm{Re}[\omega(k_0)] = 0$, $\mathrm{Im}[\omega(k_0)] = 0$, stationary pattern formation.

Our object is to look for the set of valid maxima of the wave numbers k_0 for which the system may exhibit absolute or convective instability, or stationary pattern formation for the respective values of the constant current density j (here onwards referred to as the $j - k_0$ space). As mentioned earlier, this current density j can be controlled [13] from outside depending on the nature of the experiment. We discuss these cases separately in terms of the j versus k_0 plot in the following three subsections.

A. Absolute instability

When a small perturbation lifts the system to a state different from the initial, and the perturbation moves forward, transforming the system to a final state away from the steady state, it is said to be absolute instability. In the present context, when both the real as well as the imaginary part of the eigenvalues are nonzero, it implies absolute instability. The presence of the real part in the solution of the eigenvalues $\mathrm{Re}(\omega)$ signifies a nonzero imaginary time-part in the expo-

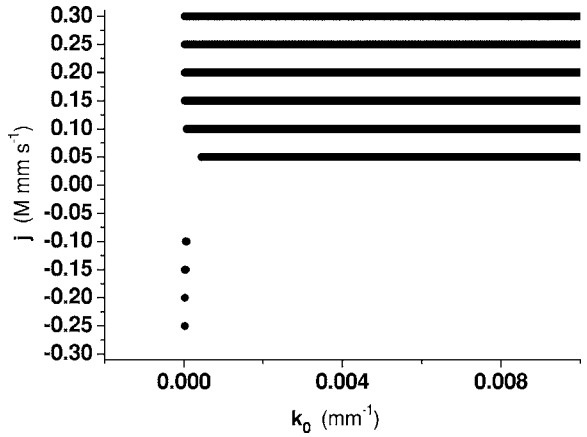

FIG. 1. The set of valid maxima of wave numbers (k_0) for each of the applied constant current density values (j), corresponding to the eigenvalues that satisfy the absolute instability condition ($\mathrm{Re}[\omega(k_0)] \neq 0, \mathrm{Im}[\omega(k_0)] \neq 0$), for the parameter set mentioned in the text.

nential part of the spatiotemporal perturbations $e^{-i\omega t}$ [Eq. (3.7)], and thus predicts the wave front propagation in the system with no back. On the other hand, the imaginary part of the eigenvalues $\mathrm{Im}(\omega)$, i.e., the real time-part in the exponential of the perturbation, promises a final state that is different from the initial state. Figure 1 identifies the $j-k_0$ space where a small perturbation would lead to absolute instability in the system.

B. Convective instability

A spatially extended system is said to be convectively unstable if a perturbation takes it away from the steady state, that propagates as a wave packet growing in size. But unlike in the case of absolute instability, in this case, when the wave packet passes by, the system comes back to the original steady state. The condition of convective instability is given by the reality of the eigenvalues ω, i.e., $\mathrm{Im}[\omega(k_0)]=0$. Figure 2 shows the $j-k_0$ space where a small perturbation would lead the system into a state of convective instability.

C. Stationary pattern

When the perturbation is constant with time, with a purely imaginary exponent, it can give rise to a stationary pattern. i.e., the exponential part should be of the form, $e^{i(k_x x+k_y y)}$, such that, $\omega=0$ and k_x and k_y are real. Figure 3 shows the $j-k_0$ space for which a perturbation may bring about a transition to a pattern stationary in time.

IV. NUMERICAL SIMULATION

We carry out numerical simulations of the reaction-diffusion system [Eqs. (2.10)–(2.12) and (2.19)], using the explicit Euler method for the integration of the equations, following the discretization of space and time. A finite system size of 100×100 grid points has been chosen. Zero flux boundary conditions have been considered for the concentration along all the four walls. As for the potential, zero-flux

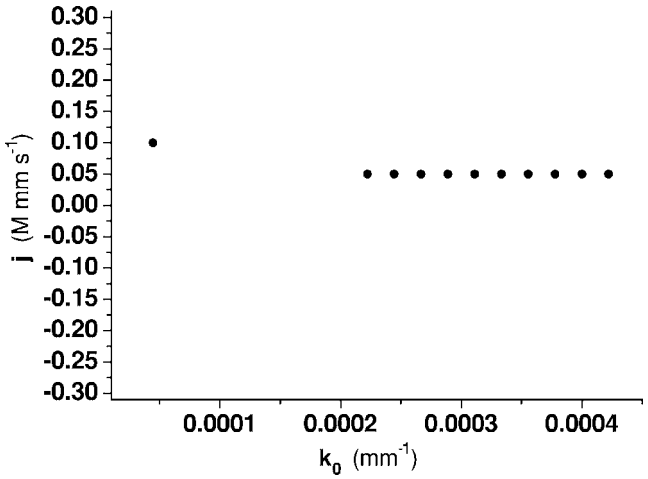

FIG. 2. The set of valid maxima of wave numbers (k_0) for each of the applied constant current density values (j), corresponding to the eigenvalues that satisfy the convective instability condition ($\mathrm{Re}[\omega(k_0)] \neq 0, \mathrm{Im}[\omega(k_0)]=0$), for the parameter set mentioned in the text.

boundary is applied at the two sides parallel to the direction of propagation of the wave-front, and a constant boundary is applied at the walls ahead and behind the front [13], as given by

$$\nabla\phi = -\frac{j}{(u_0+v_0+dw_0)}. \tag{4.1}$$

A time interval $\Delta t=0.00001$ s and a cell size $\Delta x=0.1$ mm, have been found to be appropriate for the purpose. We have carried out our numerical simulations for different values of j, ranging from -0.3 to 0.3 M mm s^{-1}. The initial conditions are taken identical to the initial experimental values of the reactants, with $u_0=1.0\times10^{-6}$ M, $v_0=0.006$ M, over the unreacted reaction surface ahead of the front. A small area behind the front, is considered as that where the reaction has

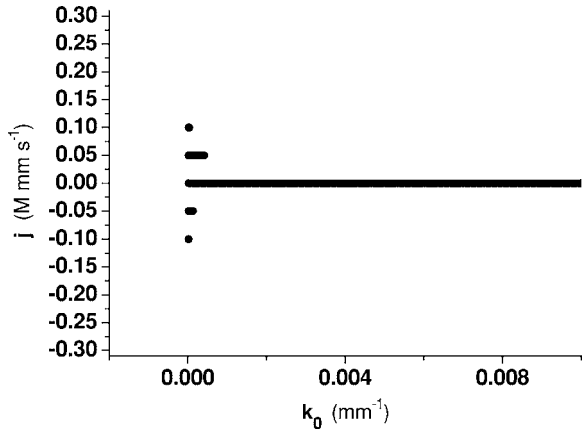

FIG. 3. The set of valid maxima of wave numbers (k_0) for each of the applied constant current density values (j), corresponding to the eigenvalues that satisfy the condition for stationary pattern formation ($\mathrm{Re}[\omega(k_0)]=0, \mathrm{Im}[\omega(k_0)]=0$), for the parameter set mentioned in the text.

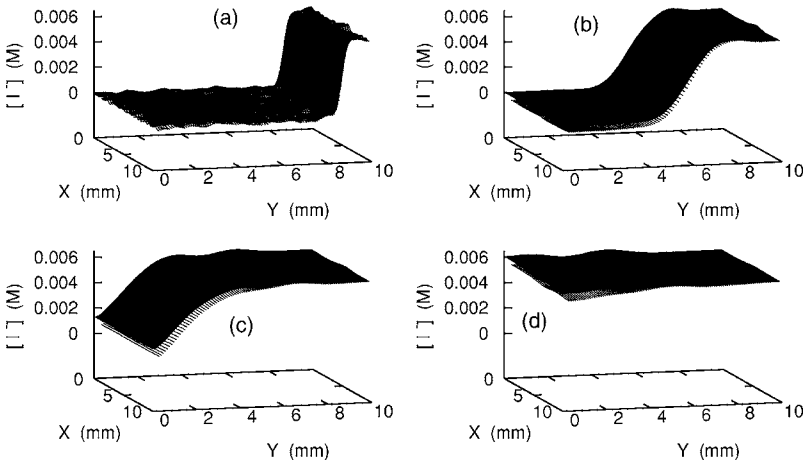

FIG. 4. Time evolved surface plots of the concentration values for the iodide ion at a constant current density of $j=0.3$ M mm s^{-1} showing absolute instability. (a) 10 s, (b) 100 s, (c) 200 s, and (d) 300 s (other parameters are as mentioned in the text).

already taken place, and the initial values of the iodide ion here is considered to be $u_0=0.006$ M, and that of the iodate, $v_0=1.0\times10^{-6}$ M. The hydrogen ion, or acid catalyst, that acts as a buffer is taken to be initially uniform all over the reaction vessel with a concentration of $w_0=0.0071$ M. The rate constants, viz. k_1 and k_2 are taken as per the experimental values mentioned earlier.

We calculate the iodine concentration at any time 't', as a function of the concentrations of iodide and iodate ions, taking into consideration of the conservation of total iodine in the system:

$$[\mathrm{I}_2]_t=\frac{1}{2}([\mathrm{I}^-]_0+[\mathrm{IO}_3^-]_0-[\mathrm{I}^-]_t-[\mathrm{IO}_3^-]_t). \tag{4.2}$$

In the Figs. 4 and 5, we show the surface plot of the iodide ion concentration, changing with time, to show the absolute instability arising in the system. As the wave packet moves forward it forms a concentration gradient of the reactants, as shown in the figures. The reactant concentration behind the wave front may increase to a constant value as seen in the case of absolute instability (Fig. 4). For a negative flux, the wave front shows an interesting formation, with the probable culmination of a set of backward-propagating waves with high velocity (Fig. 5). This may be explained in the following way. When the wave moves in an electric field, the I^- ions migrate towards the positive electrode. In the presence of a negative electric field, the flow of I^- ions is in the direction of propagation of the wave. This leads to a faster reaction and a sharp decrease in the concentration of I^-, resulting in a backward propagating wave (I^- wave) with high velocity, which leaves the system in a homogeneous state. On the other hand, when the flux is positive, the negatively charged iodide ions are attracted towards the anode behind the wave front and since this acts in a direction opposite to that of the wave propagation, it results in a retardation of the reaction ahead of the front, thus leading to a comparative decrease in the velocity of the wave.

In the case of convective instability, the wave-front moves forward with a maximum, and the concentration behind the wave front decreases with time. This is displayed by the surface-plot of iodine concentration (Fig. 6). The physical origin of the maximum may be traced in the nature of the $j-k_0$ plot (Fig. 2). It appears that only a sparse set of k_0 values are allowed for the constant applied current density values of j. This, in turn, implies that a few modes are selected for the wave propagation, the relative dominance between them being determined by the boundary conditions.

We plot the contour values of the iodine concentration (Fig. 7), in order to show the evolution of patterns. In Fig. 7 we have depicted the case for zero flux. Dark colors represent a greater concentration of iodine, thus representing more product formation. The pattern inhomogeneous in space, reaches stationarity around a time beyond 250 s.

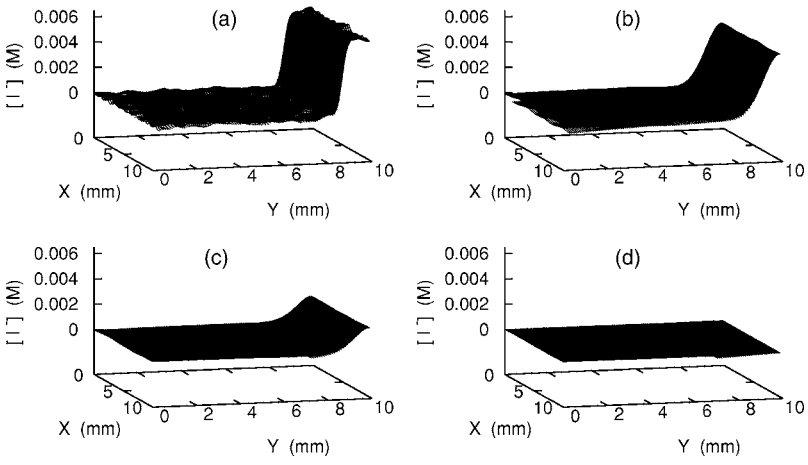

FIG. 5. Time evolved surface plots of the concentration values for the iodide ion at a constant current density of $j=-0.1$ M mm s^{-1} showing absolute instability. (a) 10 s, (b) 100 s, (c) 200 s, and (d) 300 s (other parameters are as mentioned in the text).

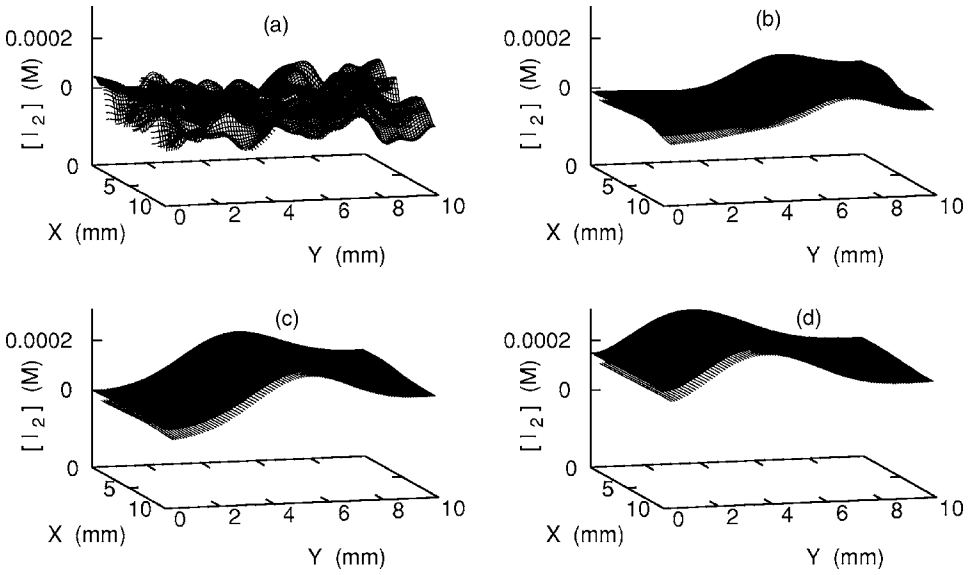

FIG. 6. Time evolved surface plots of the concentration values for iodine at a constant current density of $j=0.05$ M mm s^{-1} showing convective instability. (a) 10 s, (b) 100 s, (c) 200 s, and (d) 300 s (other parameters are as mentioned in the text).

We also observe the variation of the time ($t_{1/2}$) required by the system to reach half of the final concentration $\left[u(x_a,y_a)=\frac{1}{2}u_0\right]$ for the forward propagating waves (positive j) at some particular predetermined point (x_a,y_a) ahead of the wave front, and half of the initial concentration $\left[u(x_b,y_b)=\frac{1}{2}u_0\right]$ for the backward propagating waves (negative j) at some particular point (x_b,y_b) behind the wave front, such that (x_a,y_a) and (x_b,y_b) are equidistant from the initial position of the wave front. Or in other words, the time of wave travel $t_{1/2}$, that has been simulated gives us only a measurement of the time required by the propagating wave front to reach a particular point. The initial conditions have been set as in the previous case. It can be seen from a plot of $t_{1/2}$ V s. j (Fig. 8), that $t_{1/2}$ varies hyperbolically with respect to j, with asymptotes at $x=0$ and $y=0$; the graphs for positive and negative j forming a pair of conjugate rectangular hyperbolas, with only a valid positive y axis (time axis). This gives a graphical measure of the velocity of the wave front, that changes with variation of flux j. As j becomes more and more negative, the propagation velocity increases rapidly. On the other hand, the propagation velocity is nearly zero for $j=0.0$ M mm s^{-1} and very low values of j, which again increases as the flux moves to higher positive values. The hyperbola around $j=0.0$ M mm s^{-1} is in coherence with the analytical result that for both positive and negative values of flux, the wave propagates, while for zero flux, we observe that $t_{1/2}$ is almost infinity, signifying the formation of patterns stationary in time.

As concentration of iodide at a point decreases with time, the electric field also varies in time. This has been shown in Fig. 9(a). The space inhomogeneity can also be seen by plotting the electric field over the entire space at any particular time [Fig. 9(b)].

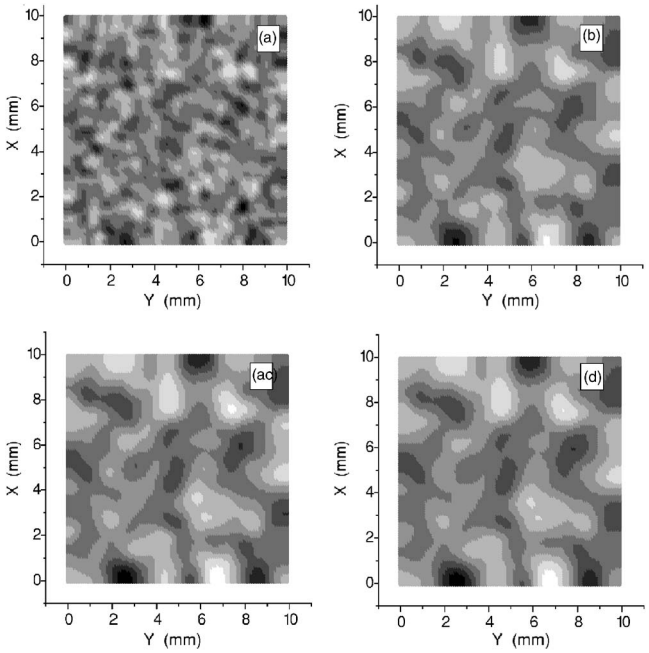

FIG. 7. Time evolved contour plots of the concentration values for iodine in the absence of current density, $j=0.0$ M mm s^{-1} showing the formation of stationary pattern. (a) 10 s, (b) 100 s, (c) 200 s, and (d) 300 s (other parameters are as mentioned in the text).

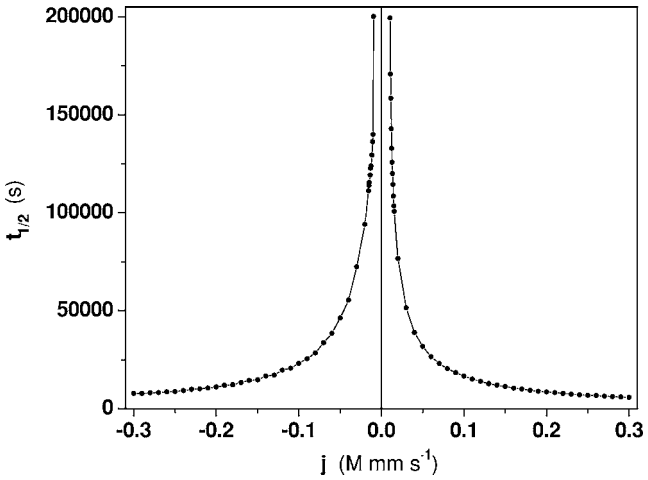

FIG. 8. Plot of $t_{1/2}$ versus j for the parameter range as mentioned in the text.

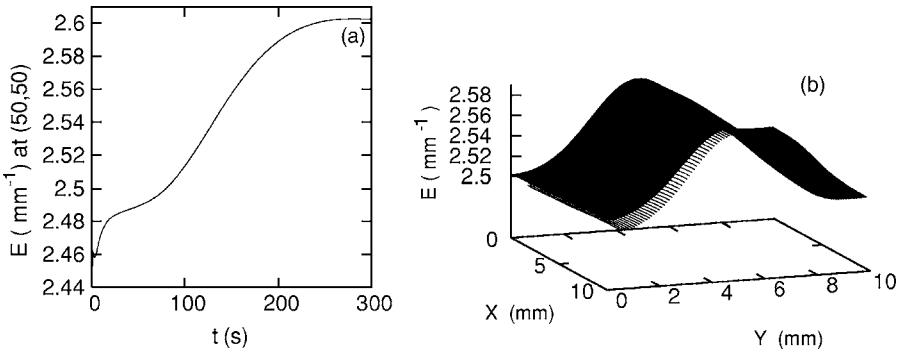

FIG. 9. (a) Plot of E versus t at (50, 50) for $j=0.05$ M mm s^{-1} and other parameters as mentioned in the text. (b) Surface plot of E at time $t=200$ s, for $j=0.05$ M mm s^{-1}.

V. CONCLUSION

We have considered in detail the inhomogeneities of the local electric field in an ionic reaction-diffusion system—the iodate-arsenous acid reaction, both analytically and numerically. The application of local charge balance condition results in convection terms which give rise to absolute and convective instabilities, appropriate for wave propagation of different types, under the influence of constant current density. The existence of stationary patterns have also been demonstrated. Our study reveals that the observations made here is also relevant in the modeling of flow-distributed oscillations where the differential flow induced instability may lead to similar situations but in a different context.

ACKNOWLEDGMENTS

Thanks are due to the Council of Scientific and Industrial Research, Government of India, for support (S.D.). One of us (S.D.) would like to thank R. K. Hazra for helpful suggestions.

APPENDIX A

The elements of the eigenvalue matrix L are as follows:

$$l_{11}=\left[-(v_0w_0^2k_1+2u_0v_0w_0^2k_2)+\frac{u_0k_x^2}{a_0}-(k_x^2+k_y^2)\right]+i\left[-\frac{u_0jk_x}{a_0^2}+\frac{jk_x}{a_0}\right], \tag{A1}$$

$$l_{12}=\left[-(u_0w_0^2k_1+u_0^2w_0^2k_2)+\frac{u_0k_x^2}{a_0}\right]+i\left[-\frac{u_0jk_x}{a_0^2}\right], \tag{A2}$$

$$l_{13}=\left[-(2u_0v_0w_0k_1+2u_0^2v_0w_0k_2)-\frac{du_0k_x^2}{a_0}\right]+i\left[-\frac{du_0jk_x}{a_0^2}\right], \tag{A3}$$

$$l_{21}=\left[\frac{v_0k_x^2}{a_0}\right]+i\left[-\frac{v_0jk_x}{a_0^2}\right], \tag{A4}$$

$$l_{22}=\left[\frac{v_0k_x^2}{a_0}-(k_x^2+k_y^2)\right]+i\left[-\frac{v_0jk_x}{a_0^2}+\frac{jk_x}{a_0}\right], \tag{A5}$$

$$l_{23}=\left[-\frac{dv_0k_x^2}{a_0}\right]+i\left[-\frac{dv_0jk_x}{a_0^2}\right], \tag{A6}$$

$$l_{31}=\left[-\frac{dw_0k_x^2}{a_0}\right]+i\left[\frac{dw_0jk_x}{a_0^2}\right], \tag{A7}$$

$$l_{32}=\left[-\frac{dw_0k_x^2}{a_0}\right]+i\left[\frac{dw_0jk_x}{a_0^2}\right], \tag{A8}$$

$$l_{33}=\left[-\frac{d^2w_0k_x^2}{a_0}-d(k_x^2+k_y^2)\right]+i\left[\frac{d^2w_0jk_x}{a_0^2}-\frac{djk_x}{a_0}\right]. \tag{A9}$$

APPENDIX B: SOLUTIONS OF ω FROM EQ. (3.18)

Let

$$G_{k_x}^a+iF_{k_x}^b=a+ib=H_{ab}\left(\frac{a}{H_{ab}}+i\frac{b}{H_{ab}}\right), \tag{B1}$$

where $H_{ab}^2=a^2+b^2$:

$$G_{k_x}^a+iF_{k_x}^b=H_{ab}(\cos\theta_{ab}+i\sin\theta_{ab})=H_{ab}e^{i\theta_{ab}}. \tag{B2}$$

Thus,

$$G_{k_x}^b+iF_{k_x}^c=H_{bc}e^{i\theta_{bc}}. \tag{B3}$$

Similarly, we have

$$G_{k_x}^c+iF_{k_x}^d=H_{cd}e^{i\theta_{cd}}. \tag{B4}$$

This gives

$$\omega_{\pm}=\frac{-H_{bc}e^{i\theta_{bc}}\pm\sqrt{H_{bc}^2e^{2i\theta_{bc}}-4H_{ab}e^{i\theta_{ab}}H_{cd}e^{i\theta_{cd}}}}{2H_{ab}e^{i\theta_{ab}}}. \tag{B5}$$

The discriminant simplifies to

$$D=H_{bc}^2e^{2i\theta_{bc}}-4H_{ab}e^{i\theta_{ab}}H_{cd}e^{i\theta_{cd}} \tag{B6}$$

$$=H_{bc}^2\cos2\theta_{bc}-4H_{ab}H_{cd}\cos(\theta_{ab}+\theta_{cd})+i[H_{bc}^2\sin2\theta_{bc}-4H_{ab}H_{cd}\sin(\theta_{ab}+\theta_{cd})]. \tag{B7}$$

Therefore D can be written as

$$D=R+iI(say). \tag{B8}$$

Thus we have

$$\omega_{\pm} = -\frac{H_{bc}(\cos\theta_{bc} + i\sin\theta_{bc})}{2H_{ab}(\cos\theta_{ab} + i\sin\theta_{ab})} \mp \frac{H_{RI}^{1/2}\left(\cos\frac{\theta_{RI}}{2} + i\sin\frac{\theta_{RI}}{2}\right)}{2H_{ab}(\cos\theta_{ab} + i\sin\theta_{ab})}, \tag{B9}$$

where $H_{RI}^2 = R^2 + I^2$ and $R + iI = H_{RI}[R/H_{RI} + i(I/H_{RI})] = H_{RI}e^{i\theta_{RI}}$. Finally $\omega_{\pm}$ are given by

$$\omega_{\pm} = -\frac{1}{2H_{ab}}\left\{H_{bc}[\cos(\theta_{bc} - \theta_{ab}) + i\sin(\theta_{bc} - \theta_{ab})] \mp H_{RI}^{1/2}\left[\cos\left(\frac{\theta_{RI}}{2} - \theta_{ab}\right) + i\sin\left(\frac{\theta_{RI}}{2} - \theta_{ab}\right)\right]\right\}. \tag{B10}$$

[1] H. Ševčíková and M. Marek, Physica D **9**, 140 (1983).
[2] S. Schmidt and P. Ortoleva, J. Chem. Phys. **67**, 3771 (1977).
[3] R. A. Gray, O. A. Mornev, J. Jalife, O. V. Aslanidi, and A. M. Pertsov, Phys. Rev. Lett. **87**, 168104 (2001).
[4] M. Hoyuelos, D. Walgraef, P. Colet, and M. San Miguel, Phys. Rev. E **65**, 046620 (2002).
[5] J. Keener and J. Sneyd, *Mathematical Physiology* (Springer-Verlag, New York, 1998).
[6] M. D. Johnson, X. Duan, B. Riley, A. Bhattacharya, and W. Luo, Phys. Rev. E **69**, 041501 (2004).
[7] M. Yang, C. S. Ozkan, and H. Gao, J. Assoc. Lab. Autom. **8**, 86 (2003).
[8] S. S. Riaz, S. Kar, and D. S. Ray, Physica D **203**, 224 (2005).
[9] S. Schmidt and P. Ortoleva, J. Chem. Phys. **71**, 1010 (1979).
[10] S. Schmidt and P. Ortoleva, J. Chem. Phys. **74**, 4488 (1981).
[11] H. Ševčíková, M. Marek, and S. C. Müller, Science **257**, 951 (1992).
[12] S. S. Riaz, S. Kar, and D. S. Ray, J. Chem. Phys. **121**, 5395 (2004).
[13] Z. Virányi, Á. Tóth, and D. Horváth, Chem. Phys. Lett. **401**, 575 (2005).
[14] A. F. Münster, P. Hasal, D. Šnita, and M. Marek, Phys. Rev. E **50**, 546 (1994).
[15] F. Sagués and I. R. Epstein, J. Chem. Soc. Dalton Trans., **7**, 1201 (2003).
[16] S. Dutta, S. S. Riaz, and D. S. Ray, Phys. Rev. E **71**, 036216 (2005).
[17] A. Hanna, A. Saul, and K. Showalter, J. Am. Chem. Soc. **104**, 3838 (1982).
[18] D. Horváth and K. Showalter, J. Chem. Phys. **102**, 2471 (1995).
[19] J. H. Merkin and H. Ševčíková, Phys. Chem. Chem. Phys. **1**, 91 (1999).
[20] L. Forštová, H. Ševčíková, M. Marek, and J. H. Merkin, J. Phys. Chem. A **104**, 9136 (2000).
[21] L. Forštová, H. Ševčíková, and J. H. Merkin, Phys. Chem. Chem. Phys. **4**, 2236 (2002).
[22] S. Dushman, J. Phys. Chem. **8**, 453 (1904).
[23] J. R. Roebuck, J. Phys. Chem. **6**, 365 (1902).
[24] Stephen K. Scott, *Oscillations, Waves, and Chaos in Chemical Kinetics* (Oxford University Press, New York, 1994).
[25] G. Schmitz, Phys. Chem. Chem. Phys. **2**, 4041 (2000).
[26] I. R. Epstein and J. A. Pojman, *An Introduction to Nonlinear Chemical Dynamics* (Oxford University Press, New York, 1998).
[27] J. Newman, *Electrochemical Systems* (Prentice Hall, Princeton, NJ, 1991).
[28] J. R. Bamforth, S. Kalliadasis, J. H. Merkin, and S. K. Scott, Phys. Chem. Chem. Phys. **2**, 4013 (2000).